Photon echoes of terbium in lithium yttrium fluoride
by Paula Louise Fisher Darejeh

A thesis submitted in partial fulfillment of the requirements for the degree of Master of Science in Physics
Montana State University

Abstract:
The photon echo experiment is a method of measuring the homogeneous dephasing time (T2) from which the homogeneous linewidth of an optical transition can be calculated. In this thesis, the theories of linewidths of transitions and of the development of a photon echo are presented. Also discussed is the experimental setup by which the first photon echoes in the rare-earth terbium were observed and measured. The decays of echo intensity with laser pulse separation at the externally applied fields of 45 KG and 25 KG were plotted and from these plots a homogeneous dephasing time of HO nanoseconds was calculated. Data at 15 KG were taken, but because of the non-exponential behavior of the decay, Tj was not calculated. At 0 KG, no echo was observed, implying a decrease of the dephasing time below 15 KG.

PHOTON ECHOES OF TERBIUM IN LITHIUM YTTRIUM FLUORIDE

by

Paula Louise Fisher Darejeh

A thesis submitted in partial fulfillment
of the requirements for the degree

of

Master of Science

in

Physics

MONTANA STATE UNIVERSITY
Bozeman, Montana

December 1983

APPROVAL

of a thesis submitted by

Paula Louise Fisher Darejeh

This thesis has been read by each member of the thesis committee and has been found to be satisfactory regarding content, English usage, format, citations, bibliographic style, and consistency, and is ready for submission to the College of Graduate Studies.

Nov 28, 1983
Date

Rufus L. Cone
Chairperson, Graduate Committee

Approved for the Major Department

Nov 28, 1983
Date

Head, Major Department

Approved for the College of Graduate Studies

11-29-83
Date

Michael Malone
Graduate Dean

STATEMENT OF PERMISSION TO USE

In presenting this thesis in partial fulfillment of the requirements for a master's degree at Montana State University, I agree that the library shall make it available to borrowers under rules of the Library. Brief quotations from this thesis are allowable without special permission, provided that accurate acknowledgement of source is made.

Permission for extensive quotation from or reproduction of this thesis may be granted by my major professor, or in his absence, by the Director of Libraries, when in the opinion of either, the proposed use of the material is for scholarly purposes. Any copying or use of the material in this thesis for financial gain shall not be allowed without my written permission.

Paula Louise Fisher Darrah
Signature

November 28, 1983
Date

TABLE OF CONTENTS

LIST OF FIGURES

LIST OF FIGURES - Continued

ABSTRACT

The photon echo experiment is a method of measuring the homogeneous dephasing time (T_2) from which the homogeneous linewidth of an optical transition can be calculated. In this thesis, the theories of linewidths of transitions and of the development of a photon echo are presented. Also discussed is the experimental setup by which the first photon echoes in the rare-earth terbium were observed and measured. The decays of echo intensity with laser pulse separation at the externally applied fields of 45 KG and 25 KG were plotted and from these plots a homogeneous dephasing time of 110 nanoseconds was calculated. Data at 15 KG were taken, but because of the non-exponential behavior of the decay, T_2 was not calculated. At 0 KG, no echo was observed, implying a decrease of the dephasing time below 15 KG.

CHAPTER 1

INTRODUCTION

The first observation of the phenomenon known as photon echoes was reported by I. D. Abella, N. A. Kurnit, and S. R. Hartmann at Columbia University in 1964[1]. That group performed an experiment "in which a ruby crystal has been made to emit spontaneously a short, intense burst of radiation, which we will call a photon echo ...". In later analysis[2] by the same group predictions of echo intensity, echo polarization, and direction of echo propagation were derived utilizing Dicke's theory of "super-radiant states"[3]. The echo was foundto decay exponentially as a function of separation between the excitation pulses with a decay time proportional to T_2, the homogeneous dephasing time of the excited state. If one of the energy levels of the echo transition was nearly degenerate[4], for example if split by hyperfine interactions, then superimposed upon the exponential decay would be a modulation with period inversely proportional to the splitting. Thus, from the behavior of the echo intensity as a function of pulse separation, information about the homogeneous linewidth

(which is inversely proportional to T_2) of the echo transition and about the hyperfine splittings of the involved energy levels could be extracted. The photon echo experiment can thus extract information usually masked by the broad inhomogeneous linewidths of non-isolated atoms. Numerous applications of the photon echo experiment have been reported in gases[5], in organic molecules[6], and in rare-earth doped crystals [7].

This thesis reports on the first observation and measurement of photon echoes in the rare-earth terbium ion. The significance of this experiment is due to several factors:

(1) The linewidths of terbium transitions have not previously been studied in any detail. In particular, mechanisms of homogeneous broadening are only speculative at this time.

(2) This experiment could directly show any hyperfine splittings or other structure of energy levels on a scale unresolvable by other experiments.

Chapters 2 through 4 of this thesis are devoted to the theories which provide the basis for understanding this experiment. In the second chapter, the theories of homogeneous and inhomogeneous broadening and the mechanisms of each are presented. The third chapter

contains the mathematical prediction of photon echoes, followed by a less formal physical discussion of how the echo arises. The laser intensities required to produce an echo are also calculated. In the fourth chapter, the terbium ion's structure and allowed transitions in the crystal environment are presented. Chapter 5 describes the experimental setup and chapter 6 describes each component of the setup in detail. Chapter 7 describes a complete experimental run. The eighth chapter contains the relevant data, the analysis of that data, and the conclusion drawn about the homogeneous linewidth and structure (or lack of structure) of the $^7F_6 - {}^5D_4\Gamma_1$ transition in terbium.

CHAPTER 2

HOMOGENEOUS AND INHOMOGENEOUS LINEWIDTHS

In an ensemble of two-level atoms, the wavefunction of each atom can be written as a superposition

$$\Psi(\bar{r},t) = c_1(t)u_1(\bar{r}) + c_2(t)u_2(\bar{r}) = \sum_n c_n u_n \qquad \text{Eq. 1}$$

where $c_n(t) = \langle u_n(\bar{r}) | \Psi(\bar{r},t) \rangle$ and $Hu_n = E_n u_n$. $|c_1|^2$ or $|c_2|^2$ is the probability that the atom is in the lower state or upper state, respectively.

For the ensemble, the general density operator is defined as

$$\rho = \sum_j P_j |\Psi_j\rangle\langle\Psi_j| \qquad \text{Eq. 2}$$

where P_j is that fraction of atoms which has the state vector Ψ_j. Using equation 1 for Ψ, we get

$$\rho = \sum_j P_j \sum_n \sum_m c_n{}^{(j)} c_m{}^{*(j)} |u_n\rangle\langle u_m| = \sum_{nm} \rho_{nm} |u_n\rangle\langle u_m|$$

where ρ_{nm} has been defined as

$$\rho_{nm} = \sum_j P_j c_n{}^{(j)} c_m{}^{*(j)} = \overline{c_m{}^* c_n} \qquad \text{Eq. 3}$$

Thus, for an ensemble of two-level atoms, the density matrix is

$$\rho = \sum_j P_j \begin{pmatrix} |c_1(j)|^2 & c_1(j)c_2^*(j) \\ c_2(j)c_1^*(j) & |c_2(j)|^2 \end{pmatrix} \qquad \text{Eq. 4}$$

For the ensemble of two-level atoms, ρ_{ii} is the probability of finding an atom of the ensemble in the i^{th} state. If N is the density of atoms, then $N(\rho_{11}-\rho_{22})$ is the average density of the population difference between the two levels.

For an electric dipole interaction Hamiltonian, $V = \mu E(t)$, with $\mu_{11} = \mu_{22} = 0$ and $\mu_{12} = \mu_{21} = \mu$. The ensemble average $\overline{\langle\mu\rangle} = tr(\rho\mu) = \mu(\rho_{12} + \rho_{21})$. But since $\rho_{12} = \rho_{21}^*$

$$\overline{\langle\mu\rangle} = \mu(\rho_{21} + \rho_{21}^*). \qquad \text{Eq. 5}$$

The macroscopic polarization is given by

$$P = N\,\overline{\langle\mu\rangle}.$$

Taking the partial derivative of equation 2 with respect to time, we obtain

$$\frac{\partial\rho}{\partial t} = \sum P_j\left[|\dot{\Psi}_j\rangle\langle\Psi_j| + |\Psi_j\rangle\langle\dot{\Psi}_j|\right] \qquad \text{Eq. 6}$$

From Schrodinger's equation, $|\dot{\Psi}\rangle = -\frac{i}{\hbar} H |\Psi\rangle$ Eq. 7

Taking the hermitian conjugate and noting that H is hermitian

$$\left[|\dot{\Psi}\rangle\right]^t = \left[-\frac{i}{\hbar} H|\Psi\rangle\right]^t$$

$$\langle\dot{\Psi}| = +\frac{i}{\hbar}\langle\Psi|H \qquad \text{Eq. 8}$$

Using equations 7 and 8 in equation 6, we get

$$\frac{\partial\rho}{\partial t} = -\frac{i}{\hbar}\sum P_j\left[\, H|\Psi_j\rangle\langle\Psi_j| + |\Psi_j\rangle\langle\Psi_j|H \,\right]$$

Therefore,

$$\frac{\partial\rho}{\partial t} = -\frac{i}{\hbar}\left[\, H,\rho \,\right] \qquad \text{Eq. 9}$$

if H is the same for all $|\Psi\rangle$.

The Hamiltonian describing the internal energies of the atoms and the interaction between the atoms and the electric field is $H = H_o + V$. Here, H is taken to be the same for all atoms. H_o is the unperturbed Hamiltonian which describes the internal energies of the atoms ($H_o u_n = E_n u_n$). V is the dipole interaction Hamiltonian (V =

$-E(t)\mu$). The matrix representations of the operators H_o, ρ, and μ are

$$H_o = \begin{pmatrix} E_1 & 0 \\ 0 & E_2 \end{pmatrix}, \quad \rho = \begin{pmatrix} \rho_{11} & \rho_{12} \\ \rho_{21} & \rho_{22} \end{pmatrix}, \quad \text{and} \quad \mu = \begin{pmatrix} 0 & \mu \\ \mu & 0 \end{pmatrix}$$

Thus, equation 9 for the time evolution of the density matrix yields the following formulas

$$\frac{\partial \rho_{21}}{\partial t} = -\frac{i}{\hbar}\left[H, \rho \right]_{21}$$

$$= -\frac{i}{\hbar}\left[(H_o\rho)_{21} + (V\rho)_{21} - (\rho H_o)_{21} - (\rho V)_{21} \right]$$

$$= -\frac{i}{\hbar}\left[E_2\rho_{21} - E(t)\mu\rho_{11} - E_1\rho_{21} + E(t)\mu\rho_{22} \right]$$

$$\frac{\partial \rho_{21}}{\partial t} = -i\omega_o\rho_{21} + i\mu E(t)(\rho_{11} - \rho_{22})/\hbar \qquad \underline{\text{Eq.10}}$$

where $\omega_o = (E_2 - E_1) / \hbar$.

Using the normalization condition $\rho_{11} + \rho_{22} = 1$ and using the same approach given above, we find

$$\frac{\partial}{\partial t}(\rho_{11} - \rho_{22}) = 2i\mu E(t)(\rho_{21} - \rho_{21}^{*}) \qquad \underline{\text{Eq.11}}$$

In the absence of an electric field, equation 10 has the solution

$$\rho_{21} = \rho_{21}^{o} \, e^{-i\omega_o t} \qquad \text{Eq.12}$$

At this point the effect of random dephasing of the atoms has to be included. When E(t) is turned off, we would expect that ρ_{21} would decrease and eventually approach zero as the relative phase coherence is lost due to random inelastic collisions with phonons and other random effects. Thus for the ensemble, equation 12 should become

$$\rho_{21} = \rho_{21}^{o} \, e^{(-i\omega_o t - t/T_2)}$$

where T_2 is the dephasing time. Equation 10 is then modified to include the dephasing and becomes

$$\frac{\partial \rho_{21}}{\partial t} = - i\omega_o \rho_{21} + i\mu E(t)(\rho_{11} - \rho_{22})/\hbar - \rho_{21}/T_2 \qquad \text{Eq.13}$$

In a similar manner, equation 11 is modified to include the relaxation of the population difference $N(\rho_{11} - \rho_{22})$ to its equilibrium value $N(\rho_{11} - \rho_{22})_o$ with a time constant τ.

$$\frac{\partial}{\partial t}(\rho_{11}-\rho_{22}) = \frac{2i\mu E(t)}{\hbar}(\rho_{21}-\rho_{21}^{*}) - \frac{(\rho_{11}-\rho_{22})-(\rho_{11}-\rho_{22})_o}{\tau}$$

Eq.14

For an electric field of the form $E(t) = E \cos \omega t$ and defining the slowly varying variables

$$\sigma_{12}(t) = \sigma_{21}^{*}(t) = \rho_{12}(t)e^{-i\omega t} \qquad \text{Eq.15}$$

we obtain from equations 13 and 14 the optical Bloch equations

$$\frac{\partial \sigma_{21}}{\partial t} = -i(\omega-\omega_o)\sigma_{21} + \frac{i\mu E(t)}{2\hbar}(\rho_{11}-\rho_{22}) - \frac{\sigma_{21}}{T_2} \qquad \text{Eq.16}$$

$$\frac{\partial}{\partial t}(\rho_{11}-\rho_{22}) = \frac{i\mu E(t)}{\hbar}(\sigma_{21}-\sigma_{21}^{*}) - \frac{(\rho_{11}-\rho_{22})-(\rho_{11}-\rho_{22})_o}{\tau} \qquad \text{Eq.17}$$

where terms which vary as $e^{\pm 2i\omega t}$ have been dropped. Equations 16 and 17 yield

$$\text{Im } \sigma_{21} = \frac{\Omega T_2(\rho_{11}-\rho_{22})_o}{1 + (\omega-\omega_o)^2 T_2^{\,2} + 4\Omega^2 T_2 \tau} \qquad \text{Eq.18}$$

$$(\rho_{11}-\rho_{22}) = (\rho_{11}-\rho_{22})_o \frac{1 + (\omega-\omega_o)^2 T_2^{\,2}}{1 + (\omega-\omega_o)^2 T_2^{\,2} + 4\Omega^2 T_2 \tau} \qquad \text{Eq.19}$$

Combining equations 5, 6, and 15, the macroscopic polarization is found to be

$$P = \mu(\sigma_{21}\, e^{-i\omega t} + \sigma_{21}^{*}\, e^{i\omega t})$$

which can be rewritten as

$$P = 2\mu(\mathrm{Re}[\sigma_{21}(t)]\cos\omega t + \mathrm{Im}[\sigma_{21}(t)]\sin\omega t) \qquad \text{Eq.20}$$

The macroscopic polarization is related to the complex atomic susceptibility X by

$$P = \mathrm{Re}[\varepsilon_o X E_o e^{i\omega t}] = E_o(\varepsilon_o \mathrm{Re}[X]\cos\omega t + \varepsilon_o \mathrm{Im}[X]\sin\omega t) \qquad \text{Eq.21}$$

So the imaginary part of the complex susceptibility is found from equations 18, 20, and 21 to be

$$\mathrm{Im}\ X = \frac{\mu^2 T_2 \Delta N_o}{\varepsilon_o \hbar} \frac{1}{1 + (\omega-\omega_o)^2 T_2^{\,2} + 4\Omega^2 T_2 \tau}$$

where the precession frequency Ω is defined by $\Omega = \mu E_o / 2\hbar$.

The population difference per unit volume from equation 19 is

$$\Delta N = \Delta N_o \frac{1 + (\omega-\omega_o)^2 T_2^{\,2}}{1 + (\omega-\omega_o)^2 {}_2^{\,2} + 4\Omega^2 T_2 \tau}$$

Thus,

$$\mathrm{Im}\ X \sim \Delta N \frac{T_2}{1 + 4\pi^2 (f-f_o)^2 T_2^{\,2}}$$

which has a full width at half maximum $\Delta f = (\pi T_2)^{-1}$. Thus the absorption, which is proportional to Im X, has a

full-width at half maximum of $(\pi T_2)^{-1}$. This width, called the homogeneously broadened linewidth, is due to the loss of atomic coherence due to random effects such as spin flips, collisions, transitions to other levels, etc. In this case the atoms are considered indistinguishable and have the same transition energy E_2-E_1. In the case where the atoms are distinguishable, inhomogeneous broadening occurs. This broadening reflects a spread in the individual transition energies of the atoms due to the different crystalline environment of each atom. Usually this spread in frequency is much larger than the homogeneous linewidth so it is the dominant feature in the absorption spectrum. When inhomogeneous broadening is present, conventional absorption spectroscopy cannot be used to study homogeneous linewidth. As will be shown in chapter 3, the photon echo experiment is a method of directly measuring T_2 from which the homogeneous linewidth can be calculated.

CHAPTER 3

PHOTON ECHO

Formation of the Echo

Without an externally applied radiation field, the Hamiltonian for an n-atom ensemble can be written as[3]

$$H = H_o + E \sum_{j=1}^{n} R_{j3} .$$

H_o represents the translational energy of the ensemble and the interaction energies between atoms. It will not be discussed here.

ER_{j3} is the internal energy of the $j^{\underline{th}}$ atom and has eigenvalues $\pm\frac{1}{2}E$. We can write the internal energy portion of the ensemble eigenfunction as

$$\begin{array}{lcccccccc} & j=1 & 2 & 3 & 4 & 5 & 6 & \cdots &) \\ \Psi = (& + & + & - & + & - & - & \cdots &) \end{array}$$

where a + or − sign in the $j^{\underline{th}}$ place refers to the $j^{\underline{th}}$ atom being in the excited or ground state, respectively.

R_{j3} is an operator analogous to one of the Pauli spin operators. It operates on the plus or minus sign in the $j^{\underline{th}}$ place and has the eigenvalue +1/2 or −1/2 depending

on whether the atom is in the excited or ground state. Dicke introduces three R_j operators analogous to the three Pauli spin operators and having the following properties:

$$R_{j1}(\cdots \overset{j}{\pm} \cdots) = \frac{1}{2}(\cdots \overset{j}{\mp} \cdots)$$

$$R_{j2}(\cdots \overset{j}{\pm} \cdots) = \pm \frac{i}{2}(\cdots \overset{j}{\mp} \cdots) \qquad \text{Eq.22}$$

$$R_{j3}(\cdots \overset{j}{\pm} \cdots) = \pm \frac{1}{2}(\cdots \overset{j}{\pm} \cdots)$$

The Hamiltonian describing the interaction between the atoms and the electric field is

$$H = -\sum_j \bar{\mu}_j \cdot \bar{E}$$

Since $\bar{\mu}_j$ is an odd operator, it has only off-diagonal elements

$$\bar{\mu}_j = \mu(\bar{x}R_{j1} + \bar{y}R_{j2})$$

where μ is a constant.

Thus, the total Hamiltonian describing the internal energies of the atoms and the interaction between the atoms and the electric field is

$$H = \sum_j (\hbar\omega_o R_{j3} - \sqrt{2}\ \mu(E_x R_{j1} + E_y R_{j2})) \qquad \text{Eq.23}$$

This form of the Hamiltonian was chosen by Abella, et al[2], so that an electric field of the form

$$E_x = E \cos \omega t \ , \quad E_y = E \sin \omega t$$

would cause transitions between the excited and ground states, whereas the opposite polarization would not. As that group stated, this choice, though arbitrary, gives general results.

If, following the example of Abella et al, we now define a pseudo-electric dipole moment and a pseudo-electric field by

$$\bar{p} = \sqrt{2}\ \mu \sum (R_{j1}\bar{x} + R_{j2}\bar{y} + R_{j3}\bar{z}) \qquad \text{Eq.24}$$

and

$$\bar{\xi} = E_x\bar{x} + E_y\bar{y} - (\hbar\omega_o / \sqrt{2}\ \mu\ )\ \bar{z} \qquad \text{Eq.25}$$

respectively, then the Hamiltonian can be expressed very simply as

$$H = - \bar{p} \cdot \bar{\xi}$$

The formula for the time dependence of any operator is

$$\frac{d\langle \bar{p} \rangle}{dt} = \frac{i}{\hbar} \left\langle \left[H , \bar{p} \right] \right\rangle + \left\langle \frac{\partial \bar{p}}{\partial t} \right\rangle$$

Since $\bar{p}$ is a constant of the motion, the second term is zero, and we are left with the following formula:

$$\frac{d\langle \bar{p} \rangle}{dt} = \frac{i}{\hbar} \left\langle \left[H , \bar{p} \right] \right\rangle$$

We can solve individually for each component

$$\frac{d\langle p_x \rangle}{dt} = \frac{i}{\hbar} \left\langle \left[H, p_x \right] \right\rangle \quad , \text{ etc.} \qquad \underline{\text{Eq.26}}$$

Equations 23, 24, 25, and 26, together with the commutators for the R_j's, i.e.,

$$[R_{j\alpha}, R_{j'\beta}] = iR_{j\gamma}\delta_{jj'}\varepsilon_{\alpha\beta\gamma}$$

where $\varepsilon_{\alpha\beta\gamma} = \pm 1$ depending on whether $\alpha\beta\gamma$ is an even or odd permutation of the integers, and $\varepsilon_{\alpha\beta\gamma} = 0$ when two or more indices are repeated, will be used to find $d\langle \bar{p} \rangle / dt$.

$$[H, p_x] = H\,p_x - p_x\,H$$

$$= \Big[\sum_j [\hbar\omega_o R_{j3} - \sqrt{2}\mu(E_x R_{j1} + E_y R_{j2})]\Big] \circ \Big[\sqrt{2}\mu \sum_{j'} R_{j'1}\Big]$$
$$- \sqrt{2}\mu \Big[\sum_{j'} R_{j'1}\Big] \circ \Big[\sum_j [\hbar\omega_o R_{j3} - \sqrt{2}\mu(E_x R_{j1} + E_y R_{j2})]\Big]$$

$$[H, p_x] = \sqrt{2}\mu \sum_{jj'} \big[\hbar\omega_o (R_{j3}R_{j'1} - R_{j'1}R_{j3})$$
$$- \sqrt{2}\mu E_x (R_{j1}R_{j'1} - R_{j'1}R_{j1})$$
$$- \sqrt{2}\mu E_y (R_{j2}R_{j'1} - R_{j'1}R_{j2})\big]$$

$$[H, p_x] = \sqrt{2}\mu \sum_j \big[i\hbar\omega_o R_{j2} + i2\mu E_y R_{j3}\big]$$
$$= \sqrt{2}\mu(-i\xi_z p_y + i\xi_y p_z)$$

$$\frac{d\langle p_x\rangle}{dt} = \frac{i}{\hbar}\Big\langle [H, p_x] \Big\rangle = \sqrt{2}\mu \frac{i}{\hbar} \langle [-i\xi_z p_y + i\xi_y p_z] \rangle$$

$$= \frac{\sqrt{2}\mu}{\hbar} [\ \langle p_y\rangle \xi_z - \langle p_z\rangle \xi_y\ ]$$

$$\frac{d\langle p_x\rangle}{dt} = \frac{\sqrt{2}\mu}{\hbar} [\ \langle \bar{p}\rangle \times \bar{\xi}\ ]_x$$

The procedures used to obtain $d\langle p_y\rangle/dt$ and $d\langle p_z\rangle/dt$ are identical to the procedure used above. Combining the results, we obtain

$$\frac{d\langle\bar{p}\rangle}{dt} = \frac{\sqrt{2}\mu}{\hbar}\langle\bar{p}\rangle \times \bar{\xi}$$

This equation describes a vector $\bar{p}$ precessing about a field $\bar{\xi}$. It is the basic equation of motion used to describe the formation of a photon echo. First, we make a transformation which allows us to view the system from a frame of reference rotating at frequency ω, the frequency of the applied electric field.

$$\frac{d\langle\bar{p}\rangle}{dt} = \frac{\partial\langle\bar{p}\rangle}{\partial t} + \bar{\omega} \times \langle\bar{p}\rangle \qquad \text{Eq.27}$$

where $\bar{\omega} = \omega\bar{z}$. In the rotating frame of reference, the rotating transverse field $E(\bar{x}\cos\omega t + \bar{y}\sin\omega t)$ is stationary $(E\bar{x})$ so equation 27 becomes

$$\frac{\partial\langle\bar{p}\rangle}{\partial t} = \gamma\langle\bar{p}\rangle \times [E\bar{x} + \frac{(-\omega_o + \omega)}{\gamma}\bar{z}]$$

where $\gamma = \sqrt{2}\,\mu / \hbar$. If we call the quantity $(-\omega_o+\omega)/\gamma$ the

effective field ξ_{zeff}, then this equation simply describes the vector $\langle\bar{p}\rangle$ precessing about $\bar{E}x$ or $\xi_{zeff}\bar{z}$, whichever is dominant.

It is possible to include the effect of crystalline field inhomogeneities by replacing ω_o with ω_{oj} - that is, each atom has its own rate of precession corresponding to a slightly different transition energy $\hbar\omega_o$ due to its different environment.

$$\frac{\partial\langle\bar{p}\rangle}{\partial t} = \gamma\langle\bar{p}\rangle \times [\bar{E}x + \xi_{zeffj}\bar{z}] \qquad \text{Eq.28}$$

The sequence of events leading to the photon echo is as follows:

1) Initially, the system is in equilibrium, there is no externally applied electric field, and $\langle\bar{p}\rangle$ is directed along the z axis.

2) At t=0, an electric field E $>>$ $\xi_{z\ eff}$ is applied and equation 15 becomes

$$\frac{\partial\langle\bar{p}\rangle}{\partial t} = \gamma\langle\bar{p}\rangle \times \bar{E}x$$

Thus, $\langle\bar{p}\rangle$ precesses about the x axis with period $1/\gamma E$. If $\gamma ET = \pi/2$, where T is the amount of time the electric

field is applied, then after the pulse, $\langle\bar{p}\rangle$ is along the y axis (figure 1).

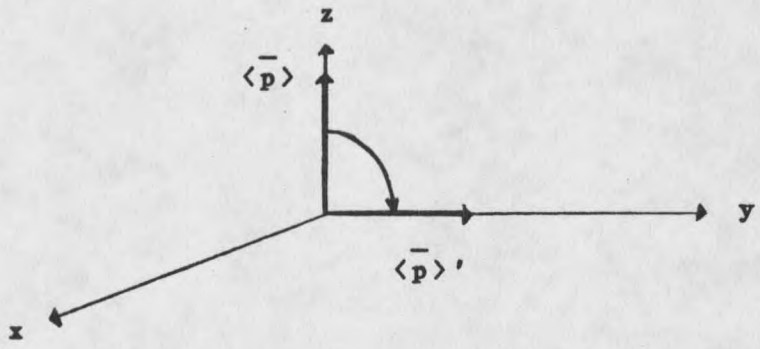

Figure 1. The precession of $\langle\bar{p}\rangle$ about $\bar{x}$.

3) Without an externally applied field $\langle\bar{p}\rangle$ is governed by the equation

$$\frac{\partial\langle\bar{p}\rangle}{\partial t} = \gamma\langle\bar{p}\rangle \times \xi_{zeffj}\bar{z}$$

and $\langle\bar{p}\rangle$ precesses about the z axis with period $\gamma\xi_{zeffj}$ (figure 2). Since each atom's period is different, the electric dipole moments quickly get out of phase with one another and the macroscopic polarization exponentially decreases.

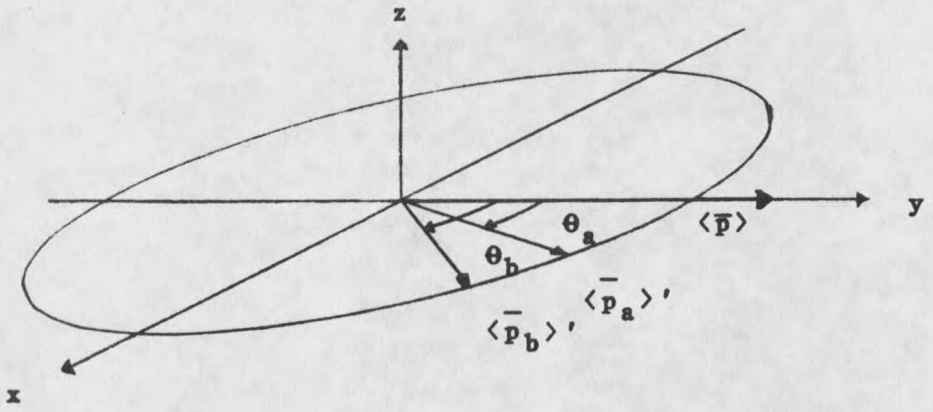

Figure 2. The precession of $\langle \bar{p} \rangle$ about $\bar{z}$.

4) At $t = \tau$, another pulse is applied, causing $\langle \bar{p} \rangle$ to again precess about the x axis (figure 3). This time, $\gamma ET = \pi$, so that each $\langle \bar{p}_j \rangle$ is reflected across the x axis, back to the x-y plane. If the angle from the y axis to $\langle \bar{p}_j \rangle$ was θ_j before the second pulse, then after the second pulse, the angle is $\pi - \theta_j$.

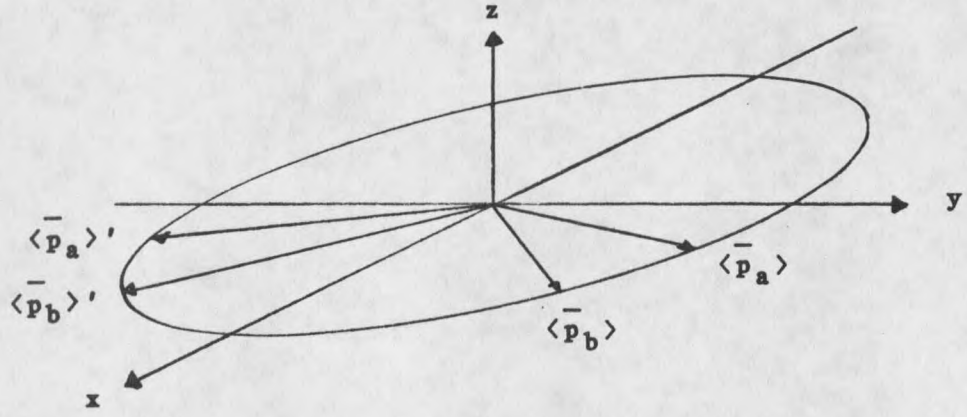

Figure 3. The precession of $\langle \bar{p} \rangle$ about $\bar{x}$.

5) After the second pulse is removed, the dipole moments again precess about the z axis with period $\gamma\xi_{zeff_j}$ (figure 4). At $t = 2\tau$, the $\langle\bar{p}_j\rangle$'s will all be along the y axis again. In the time interval τ, each $\langle\bar{p}_j\rangle$ precesses through an angle θ_j. Thus at $t = 2\tau$, the angle from the y-axis is $(\pi-\theta_j) + \theta_j = \pi$.

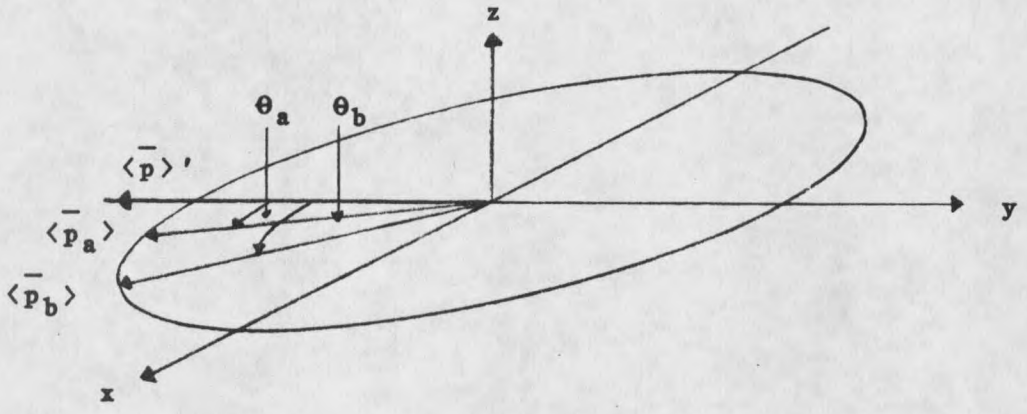

Figure 4. The precession of $\langle\bar{p}\rangle$ about $\bar{z}$.

The visual example of this sequence of events[9] involves imagining horses at a racetrack. At t=0, the gates are opened, and the horses circle the track at their respective speeds, getting out of phase. Suppose that at $t=\tau$, all the horses turn around and start running in the other direction. At $t=2\tau$, the horses are all back at the gate neck-to-neck because the slower the horse was, the less distance it had covered.

Damping of the Photon Echo

The dephasing of the dipole moments due to each atom's unique transition frequency is a deterministic process. That is, after a time δt, two atoms with resonant frequencies differing by $\delta\omega_o$ will have a phase difference $\delta\omega_o\delta t$. It is the deterministic nature of this dephasing which allows rephasing, and thus the photon echo.

If, however, there is also a stochastic, or random, dephasing mechanism such as random collisions, the echo amplitude will be greatly diminished. Each atom's dipole moment is damped at a rate T_2 while it is dephasing and rephasing along with all the other dipoles to produce the echo. Consequently, the echo amplitude is smaller by a factor of $\exp(-2\tau/T_2)$ if 2τ is the time between the initial $\pi/2$ pulse and the echo.

Direction of Echo Propagation

Abella[2] found the radiation intensity of the photon echo in the direction $\bar{k}$ due to excitation pulses with wavevectors $\bar{k}_1$ and $\bar{k}_2$ to be

$$I(\bar{k}) = \frac{1}{4} N^2 I_o \left| \exp[i(\bar{k}+\bar{k}-2\bar{k})r] \right|_{av}^2$$

where I_o is the radiation intensity of a single atom in the direction $\bar{k}$ and N is the number of atoms in the sample. The squaring of N arises because of the coherence between atoms. $I(\bar{k})$ will be a maximum when $\bar{k} = 2\bar{k} - \bar{k}$. Thus, if the second laser beam is at an angle Θ from the first, then the echo will be at angle Θ from the second beam. In order for interference effects to be negligible, the condition

$$L\,[1/(1-\Theta^2) - 1] / \lambda_{laser} \ll 1. \qquad \text{Eq.29}$$

where L is the length of the crystal, must be met. For this experiment, L = 0.2 cm and $1/\lambda = (1.5)*(20560\ cm^{-1})$, so the condition on the angle such that the interference effects are negligible is $\Theta \ll 0.013$ rad. With a 1^o crossing angle, the angle in the crystal is

$$\Theta = \frac{1^o}{1.5} \times \frac{\pi \text{ rad}}{180^o} = 0.012 \text{ rad}$$

so interference effects are not negligible, and some echo intensity is being lost.

Laser Intensities Required For $\pi/2$ And π Pulses

From Abella, et al[2], the power density required for a $\pi/2$ pulse is

$$P/A = \pi^4 \varepsilon c\hbar / 3\lambda^3 \tau^2 W \qquad \text{Eq.30}$$

where τ is the pulse duration ($5 * 10^{-9}$ sec), ε is the square of the index of refraction, and W is the probability of transition from the excited to the ground state.

The oscillator strength for the parity - forbidden $^7F_6$ - $^5D_4$ transition in terbium is calculated from the empirical data for the absorption coefficient and inhomogeneous linewidth using the formula[10]

$$f = \frac{18mc\varepsilon_o}{\pi e^2 \hbar} \quad \frac{n}{(n^2+2)^2} \quad \frac{\alpha \, \Delta E}{N_o}$$

where n is the index of refraction, α is the absorption coefficient, ΔE is the linewidth, and N_o is the Tb^{3+} ion concentration. The value of the ratio of fundamental constants at the beginning of the equation is $8.21 * 10^{17}$ $cm^{-3}/eV\ mm^{-1}$. Thus

$$f = (8.2 * 10^{17} cm^{-1}/eV mm^{-1}) \frac{(1.5)(35.8 mm^{-1})(5 * 10^{-4} eV)}{(1.5^2+2)^2 (1.36 * 10^{22} cm^{-1})}$$

$$f = 8.9 * 10^{-9}$$

From this value of oscillator strength, the transition probability is easily calculated using the formula[11]

$$W = \frac{8\pi^2\sigma^2 e^2 f}{mc}$$

where σ is the energy difference between states (20560 cm^{-1}) and e^2/mc = c * Bohr radius = $r_o c$. So

$$W = 8\pi^2\sigma^2 r_o c f$$

$$W = 2.5/sec$$

From equation 30, the power density required for a $\pi/2$ pulse is $P/A = 0.32$ Watts/μm^2. For a beam cross - sectional area of $\pi(50\mu)^2$, the required laser power would be 2.5 KW. The power required for the π pulse is (4* 2.5KW) = 10 KW.

CHAPTER 4

TERBIUM STRUCTURE AND TRANSITIONS

The Tb^{3+} ion has 62 electrons in the shells $1s^2 2s^2 2p^6 3s^2 3p^6 3d^{10} 4s^2 4p^6 4d^{10} 5s^2 5p^6 4f^8$. The spectral lines originate from transitions within the 4f configuration. Because the eight outer electrons in the 4f configuration are shielded from the crystalline environment by the 5s and 5p closed shells, the spectral lines are nearly as sharp as those of isolated atoms.

In accordance with Hund's rule[12], the lowest energy state has S = 3, L = 3, and J = 6. Thus, the ground state of Tb^{3+} is $^7F_6$. The transition used for this echo experiment is $^7F_6 - {}^5D_4$ with an energy of $hc^{\circ}(20{,}560\ cm^{-1})$.

Because electric dipole transitions among 4f states are parity forbidden ($\Delta l \neq \pm 1$), they must be forced electric dipole transitions[13]. The physical origin of these transitions is believed to be an external perturbation of odd parity, mixing the 4f orbitals (to a small extent) with the two adjacent l-values 2 and 4. Calculation of transition strengths requires a knowledge of configuration mixing, which is difficult to determine.

However, separation of allowed and forbidden transitions can be done entirely on group - theoretical grounds. In the $LiYF_4:Tb^{3+}$ crystal, the Tb^{3+} ion is at a site having S_4 symmetry (with respect to the crystal)[14]. The selection rules for S_4 symmetry give an allowed π transition between Γ_1 states and Γ_2 states. Thus, the transition $^7F_6\Gamma_2$ - $^5D_4\Gamma_1$ is π - polarized. This is the transition used in this experiment.

CHAPTER 5

EXPERIMENTAL SETUP

A diagram of the setup for the photon echo experiment is shown in figure 5. Two pulsed nitrogen-laser-pumped dye lasers are used to stimulate optical transitions in the crystal $LiYF_4:Tb^{3+}$. The timing between the two lasers is controlled electronically and scanned automatically by a computer. The crystal is cooled to liquid-helium temperatures (1.4°K - 4°K) and surrounded by a superconducting magnet coil which can produce fields up to 60KG. The echo, which is much less intense than the stimulating laser pulses must be isolated from the scattered laser light to prevent saturation of the detector. This is accomplished by using three kinds of discrimination techniques: polarization discrimination, spatial filtering, and temporal discrimination using a Pockels cell. Each of these techniques is discussed in detail later. The echo is detected by a photomultiplier tube and the electrical signal from the PMT is sent to a boxcar averager whose gate is adjusted by the computer to remain on top of the echo during the scan of the lasers' timing. The averaged signal from the boxcar is sent to an

analog-to-digital converter which is part of the data-acquisition computer. Thus, a plot of echo intensity vs. laser pulse separation is obtained somewhat automatically.

The following chapter contains detailed descriptions of the lasers, the discrimination techniques, and the electronic and computer control of the experiment.